Available online at www.sciencedirect.com
SCIENCE DIRECT®
Journal of Organometallic Chemistry 687 (2003) 153–160
Journal of Organometallic Chemistry
www.elsevier.com/locate/jorganchem

Nickel(II) complexes of the type [RM(oxam)MR] (oxam: oxalamidinate, R = *n*-butyl, *n*-hexyl): the first binuclear *n*-alkyl nickel complexes

Michael Stollenz, Manfred Rudolph, Helmar Görls, Dirk Walther *

Institut für Anorganische und Analytische Chemie der Friedrich-Schiller-Universität Jena, August-Bebel-Straße 2, 07743 Jena, Germany

Received in revised form 14 July 2003; accepted 14 July 2003

Abstract

The reaction between one equivalent of [(acac)Ni(**A**)Ni(acac)] (**A**: N^1,N^2-bis(2-pyridylmethyl)-N^3,N^4-bis-(2,4,6-trimethylphenyl)oxalamidinate) and two equivalents of R-Li (R = *n*-butyl; *n*-hexyl) results in the formation of the binuclear complexes [(R–Ni)(**A**)(Ni–R)] (**1**: R = *n*-butyl: **2** = *n*-hexyl). Both compounds were characterized by ^{1}H- and ^{13}C-NMR spectroscopy, elemental analysis, and mass spectroscopy. X-ray single diffraction studies of single crystals of **1** and **2** show that symmetrical binuclear complexes are formed in which the two Ni(II) centers are connected by the oxalamidinato bridging ligand **A** in a planar-square environment. No agostic interactions between the β-hydrogens of the *n*-alkyl groups and the metal centers were observed. DTA- and DTG-investigations show, that **1** and **2** are surprisingly thermally stable (decomposition temperature of **1**: 188 °C under formation of butenes). Heating up a 1:1 mixture of **1** and **2** in toluene results in the formation of octane, decane and dodecane indicating an intermolecular transfer reaction of the *n*-alkyl-groups in solution. CV measurements display that the oxam complexes [(R–M)(A)(M–R)] (M = Ni, R = CH_3 (**3**), Ph (**4**), CCH (**6**), CCPh (**7**); M = Pd, R = CH_3 (**5**) are reversibly reduced in two steps indicating electronic interactions between the two metal centers.

Keywords: Nickel; Palladium; Bridging ligand; Cyclic voltammetry; Electronic communication

1. Introduction

Bi- and oligonuclear complexes containing transition metals bridged by chelating ligands which allow electronic interactions between the metals are of growing interest in catalysis [1–3]. Interesting and very variable building block ligands are the oxalic amidines and their dianions ('oxam-type ligands'). These bridging ligands can coordinate very different metals in different coordination modes [4,5].

Recently we described the first organometallics with these ligands containing late metals (Ni, Pd) [2,6,7]. Furthermore, we constructed the first tri- and tetranuclear complexes [1] in which two different metals are linked by oxam bridges. Some of these complexes are catalytically active in the Kumada cross coupling, Sonogashira reaction and in the Heck reaction [2]. Moreover, a variety of Ni complexes of this type is capable of oligomerizing/polymerizing ethylene [1,2]. In this catalytic reaction two Ni centers, situated at the periphery of the complexes, are found to be catalytically active. Therefore, in the catalytic cycle both metals should react to form reactive binuclear *n*-alkyl Ni species containing $R'(CH_2)_n$–Ni(oxam)Ni–$(CH_2)_nR'$ fragments which can undergo insertion of further ethylene molecules to form two growing carbon chains on the opposite sides of the oxam bridge. In this connection the question arises wether it is possible to isolate such types of binuclear *n*-alkyl Ni complexes which could act as model compounds for the above catalytic species.

Here we describe the synthesis, NMR spectra and solid state structure of the complexes (R–Ni)(**A**)(Ni–R) (**1**: R = *n*-butyl; **2**: *n*-hexyl; **A**: N^1,N^2-bis(2-pyridyl-

* Corresponding author. Tel.: +49-3641-948-119; fax: +49-3641-948-102.
E-mail address: cdw@rz.uni-jena.de (D. Walther).

0022-328X/03/$ - see front matter © 2003 Elsevier B.V. All rights reserved.
doi:10.1016/j.jorganchem.2003.07.021

methyl)-N^3,N^4-bis(2,4,6-trimethylphenyl)oxalamidinat). To the best of our knowledge these complexes are the first binuclear *n*-alkyl-Ni compounds which could synthesized and structurally elucidated.

Complexes **1** and **2** are remarkable thermally stable. Furthermore, electrochemical measurements confirm electronic interaction between the both Ni centers. Comparison with other σ-organo nickel complexes of the above type shows that the electronic communication between the metals strongly depends on the nature of the group R.

2. Results and discussion

2.1. Synthesis and structures of the complexes 1 and 2

Reaction of one equivalent [(acac)Ni(**A**)Ni(acac)] in THF with two equivalents *n*-butyllithium in hexane at −78 °C resulted in a dark red solution from which orange–brown crystals of **1** of the composition [(R–Ni)(**A**)(Ni–R)] (R = *n*-butyl) were obtained in 42% yield. Using *n*-hexyllithium instead of *n*-butyllithium yielded the analogous complex **2** (R = *n*-hexyl) which was isolated as a golden brown crystalline solid in 49% yield. Single crystals of **1** and **2** were grown from toluene at −18 °C. Both compounds are readily soluble in THF, toluene and benzene. It is noteworthy that complex **2** is also soluble in pentane. DTA measurements under isochoric conditions showed the remarkable high thermal stability of the complexes. Complex **1** started to decompose at 188 °C in the solid state and **2** decomposes at 186 °C (Scheme 1).

Elemental analysis and mass spectra of **1** and **2** confirmed their compositions. Both complexes **1** and **2** are diamagnetic, so their NMR spectra showed signals in the expected range for a diamagnetic binuclear complex, wherein the oxam acts as a bischelating anionic ligand. In the ^{1}H-NMR spectrum of **1**, recorded at 400 MHz in benzene-d_6 at room temperature, three signals of the *n*-butyl-groups between $\delta = -0.03$–(−0.01), 0.86–0.89 and 1.25–1.49 ppm as multiplets were found. HH-COSY experiments show that the second multiplet belongs to the methyl groups of the butyl groups. Three singlets for the methyl mesityl groups and the CH_2 groups were detected at $\delta = 2.23$, 2.75 and 3.76 ppm. The protons of the aromatic rings were found between $\delta = 5.64$ and 7.90 ppm. These results indicate that the structure of **1** is highly symmetrical in solution.

The corresponding 50 MHz–^{13}C-NMR spectrum is in agreement with this conclusion. The signals of the *n*-butyl-chains appear at $\delta = 14.0$, 14.6, 27.0 and 33.0 ppm. Furthermore, the resonances of the methyl mesityl groups were observed at 19.6 and 21.2 ppm. The CH_2 groups of the oxam ligand were detected at 52.8 ppm. In the region of the aromatic carbons the expecteted number of 10 signals were found between 120.4 and 168.2 ppm.

The molecular structure of **1** was determined by an X-ray analysis of single crystals isolated from toluene (Fig. 1). Similar to other oxam complexes [1,2,4–7], **1** consists of a bimetallic centrosymmetric unit in which the oxam ligand acts in a bis-chelating fashion to bridge two nickel centers. Each nickel atom is surrounded by three N donor atoms of the oxam ligand and the α-carbon of the *n*-butyl chain. The central N_2C–CN_2-framework is essentially planar. Typically for bimetallic centrosymmetric complexes of the oxam type the C–N bonds of this framework are almost equivalent within the experimental error (C1–N1 1.333(4) and C2–N2 1.304(4) Å) indicating a high double bond character due to the electron delocalization over the two CN_2 units. Consequently, the C–C bond between these units is that of a single bond (C1–C2 1.507(5) Å).

The two *n*-butyl-groups are coordinated at the metal centers situated on opposite sides of the oxam bridge and occupy *trans* positions to each other. The Ni1–C33 bond distance of **1** is relatively short (1.948(4) Å), but it is in the same range as the Ni–C bonds in the corresponding methyl compound **3** (1.950(3) Å [6]. The C33–C34 and C34–C35 bond lengths of 1.507(6) and 1.516(6) Å, respectively, and the corresponding bond angles C34–C33–Ni1 and C33–C34–C35 of 112.6(3) and 115.7(4)° confirm that the carbons in the *n*-butyl

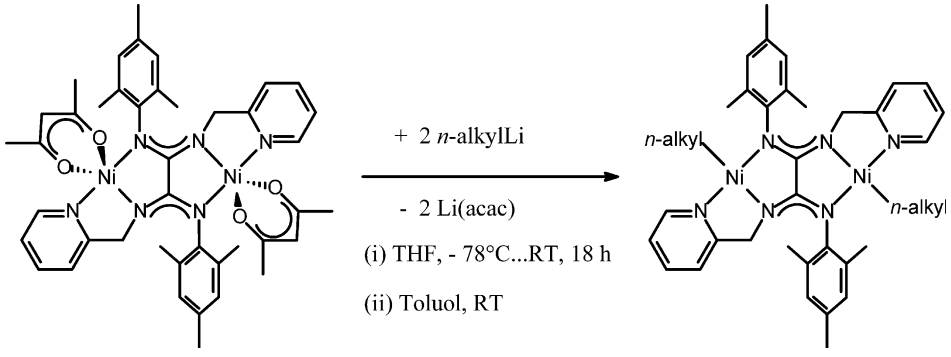

Scheme 1. Formation of the complexes **1** and **2**.

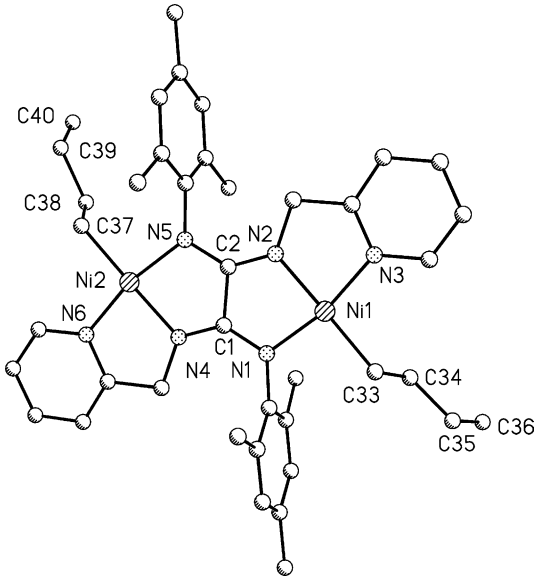

Fig. 1. Molecular structure of complex **1**. Selected bond distances (Å) and bond angles (°): Ni1–N1 1.912(3), Ni1–N2 1.901(3), Ni–N3 1.907(3), Ni1–C33 1.948(4), Ni2–N4 1.908(3), Ni2–N5 1.915(3), Ni2–N6 1.897(3), Ni2–C37 1.922(4), C1–N1 1.333(4), C1–N4 1.309(4), C2–N2 1.304(4), C2–N5 1.333(4), C1–C2 1.507(5), C33–C34 1.507(6), C34–C35 1.516(6), C35–C36 1.552(8), C37–C38 1.480(7), C38–C39 1.593(7), C39–C40 1.399(19), N1–Ni1–N2 83.3(1), N1–Ni1–N3 167.6(1), N1–Ni1–C33 96.0(1), C34–C33–Ni1 112.6(3), C33–C34–C35 115.7(4), N2–Ni1–N3 84.3(1), N2–Ni1–C33 178.1(2), N3–Ni1–C33 96.4(2), N4–Ni2–N5 83.3(1), N4–Ni2–N6 84.5(1), N4–Ni2–C37 178.3(2), N5–Ni2–N6 167.9(1), N5–Ni2–C37 95.0(1), N6–Ni2–C37 97.1(2), N1–C1–C2 114.2(3), N1–C1–N4 134.0(3), N4–C1–C2 111.8(3), C1–C2–N2 111.6(3), C1–C2–N5 114.3(3), N2–C2–N5 134.1(3).

chain are sp^3 hybridized. The molecular structure state gives no evidences for agostic interactions with the β- or γ-hydrogen of the *n*-butyl groups.

In the ^{1}H-NMR spectrum (benzene-d_6) of **2** the resonances of the *n*-hexyl chains were observed in four separated signals. The CH_2 groups were found as a separated multiplet between −0.05 and −0.01 ppm. HH-COSY experiments allow to assign the other signals with the resonances of the protons of the *n*-hexyl groups. The CH_3 groups of the *n*-Ni alkyl chains of **2** appear as a multiplet between 0.90 and 0.93 ppm. The γ-, δ-, and ε-CH_2 groups were also observed as a multiplet between 1.21 and 1.33 ppm. Furthermore, the β-CH_2 groups were found between 1.41 and 1.47 ppm. Additionally, the three singlets of the methyl mesityl groups and the bridging CH_2 groups of the oxam bridge were observed at 2.25, 2.74 and 3.75 ppm with the expected intensity ratio of 3:6:2.

The ^{13}C-NMR spectrum of **2** in benzene-d_6 also shows a simple pattern corresponding to a highly symmetrical complex. The *n*-hexyl carbon resonances appear as six separated signals. CH-COSY experiments show that the signal at 14.5 ppm belongs to the methyl group of the *n*-hexyl chain. The α-CH_2 groups were found at $\delta = 15.2$ ppm. The singlets at $\delta = 23.2$ and 32.0 and 34.1 ppm are associated with the γ-, δ- or the ε-CH_2 groups. Furthermore, at $\delta = 30.6$ ppm a singlet of the β-CH_2 groups was observed. As expected for the oxam ligand, its aliphatic resonances were found at 19.6, 21.2 and 52.8 ppm. Their aromatic signals, very close to complex **1**, appear between 120.4 and 168.2 ppm.

Single crystals of **2** suitable for an X-ray analysis were grown from toluene at −18 °C. The molecular structure is shown in Fig. 2.

Similar to complex **1**, both alkyl chains coordinating to the Ni atoms lie trans to each other. The Ni–C bond lengths are typical for a σ-bonded alkyl group (Ni1–C33: 1.931(8) Å, Ni2–C39: 1.952(8) Å). The bond lengths C33–C34 and C34–C35 (respectively C39–C40 and C40–41) (between 1.511(13) and 1.556(12) Å) are those of CC-single bonds. The bond angles C33–C34–C35 and C39–C40–C41 (114.4(8) and 113.8(8) Å) are much closer to sp^3- than to sp^2-hybridization.

Recently, Okuda et al. reported about rare earth metal complexes which contain bridging *n*-alkyl ligands with agostic interactions and their role in styrene polymerization [8].

These complexes are extremely air- and moisture-sensitive and decompose under argon at room temperature over a period of days. In contrast, the nickelorgano compounds **1** and **2** are stable under these conditions. For a few minutes no change of colour is observed, when compound **2** is handled under air. Contrary to the *n*-hexyl complex, compound **1** changes its colour from orange–brown to dark-brown. Hydrolysis of both species **1** and **2** results in the formation of *n*-butane and *n*-hexane, respectively. However, the corresponding binuclear oxam Ni–OH species could not be isolated.

In general, *n*-butyl and *n*-hexyl transition metal transition metal complexes are rare. Only a few compounds are known which have been determined by X-ray diffraction studies, namely Rh-, Ir- and Pt-containing *n*-butyl compounds have been investigated [9–12]. Girolami et al. described chromium compounds which coordinate two *n*-butyl chains at one metal center [13,14]. Recently, Cr complexes with triamidoamine ligands stabilizing methyl and *n*-butyl groups have been investigated [15]. Mononuclear nickel complexes which are able to stabilize ethyl- and *n*-butyl-groups have been described by Liang et al.; however, no X-ray diffraction studies of these compounds have been published [16]. Very little is known about such transition compounds containing *n*-hexyl groups and even less of them have been characterized completely [17–20].

2.2. Thermal reactions of *1* and *2*

Measurements of the thermal decomposition of **1** and **2** in the solid state by DTA and DTG measurements showed that compounds are surprisingly stable. Com-

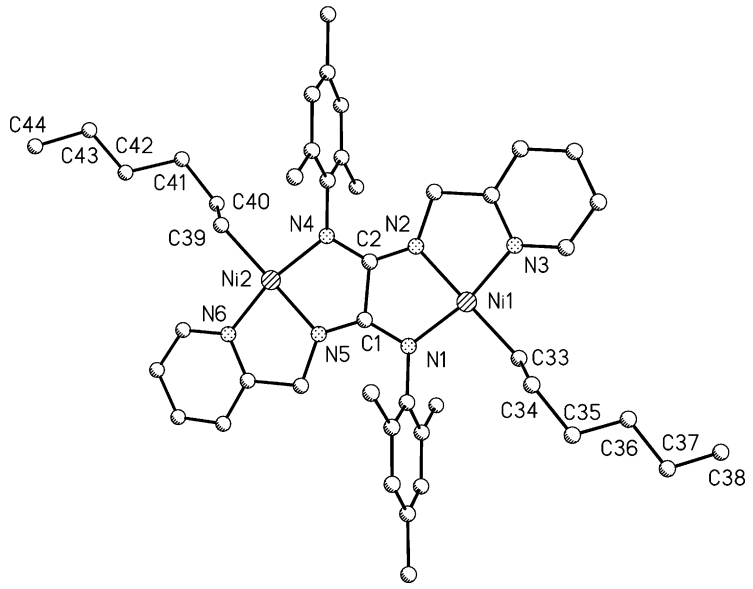

Fig. 2. Molecular structure of complex **2**. Selected bond distances (Å) and bond angles (°): Ni1–N1 1.913(7), Ni1–N2 1.928(7), Ni–N3 1.916(7), Ni1–C33 1.931(8), Ni2–N4 1.911(7), Ni2–N5 1.907(7), Ni2–N6 1.910(7), Ni2–C39 1.952(8), C1–N1 1.344(10), C1–N5 1.305(10), C2–N2 1.308(10), C2–N4 1.336(10), C33–C34 1.518(13), C34–C35 1.556(12), C35–C36 1.527(14), C36–C37 1.533(14), C37–C38 1.518(18), C39–C40 1.511(13), C40–C41 1.529(12), C41–C42 1.564(15), C42–C43 1.472(14), C43–C44 1.494(16), N1–Ni1–N2 83.5(3), N1–Ni1–N3 167.8(3), N1–Ni1–C33 96.1(3), N2–Ni1–N3 84.8(3), N2–Ni1–C33 175.8(4), N3–Ni1–C33 95.8(3), C33–C34–C35 114.4(8), N4–Ni2–N5 84.0(3), N4–Ni2–N6 167.1(3), N4–Ni2–C39 95.0(3), N5–Ni2–N6 83.9(3), N5–Ni2–C39 174.1(4), N6–Ni2–C39 97.5(3), C39–C40–C41 113.8(8), N1–C1–C2 113.9(7), N1–C1–N5 133.6(8), N5–C1–C2 112.4(7), C1–C2–N2 112.8(7), C1–C2–N4 114.4(7), N2–C2–N4 132.7(8).

plex **1** starts to decompose at 188 °C, **2** starts to decompose at 186 °C (DTA). In both cases of the DTG investigations three main stages of decomposition were observed. According to the mass lost, the first DTG peak (at 210 °C) corresponds to the eliminiation of the *n*-butyl groups in **1**. Integration of this peak area gives a loss of 14 wt.% (calculated 16 wt.%).

To investigate the reaction products given by the first decomposition stage, samples of **1** and **2** were heated in separate Schlenk tubes up to 200 °C. Under these conditions only the α-olefins 1-butene and 1-hexene, respectively were detected.

Heating solutions of both **1** and **2** in toluene under reflux gives a mixture of α-olefins and the homocoupling products *n*-octane and *n*-dodecane. This suggests that in solution the *n*-alkyl chains are eliminated not only by β-hydrogen elimination but also by homogeneous splitting of the Ni–C bonds.

Thermal decomposition in solution of a 1:1 mixture of compounds **1** and **2** should result in the formation of *n*-octane and *n*-dodecane in the ratio of about 1:1, if only an intramolecular pathway will be favoured. In case of an intermolecular reaction *n*-octane, *n*-dodecane and, in addition, *n*-decane in the ratio of about 1:1:4 should be observed.

Heating a solution of a mixture of **1** and **2** in a molar ratio of 1.0:1.1 in toluene under reflux yields α-olefins and, as expected, *n*-octane and *n*-dodecane, but also *n*-decane in a ratio of 1.0:1.2:2.1. Therefore, we suggest that the formation of the alkanes occurs mainly via an intermolecular reaction.

2.3. Electrochemical behaviour of oxam complexes

Binuclear complexes with oxam ligands are useful catalysts for some C–C linking reactions in which both metal centers can be involved in the catalytic steps. Of special interest are such reactions where the oxidation states of the metal centers change in the catalytic cycle (e.g. between +2 and 0) because the change of the oxidation states of one metal center should strongly effect the catalytic reactivity of the other metal on the opposite site of the oxam bridge.

The extent of the electronic interaction between the metals mediated by the bridging ligand is reflected in the redox potentials of the metal centers and has been measured by cyclic voltammetry. However, due to the relatively small energetic effect observed for some of the complexes the evaluation of the redox potentials of both processes from the overlapping waves could be accomplished only by fitting simulated CVs to experimental ones using the capabilities of the DIGISIM 3.0 simulation software [21]. A detailed study of the scan rate dependence of the current revealed that the experimental data are in agreement with the assumption of a simple successive two-electron reduction only when working with sufficiently high scan rates. At lower scan rates the experimental current curves associated with the second charge transfer step become significantly higher than

expected for a simple diffusion controlled process. A satisfying agreement between theory and experiment could be obtained on the basis of the ECE mechanism shown in (Scheme 2) based on the assumption that a new species 'P' is formed by the twofold reduced complex in a chemical follow-up reaction. It can be excluded from the scan rate dependence of the current signal that the chemical follow-up reaction results in a simple catalytic regeneration of complex a or b even though the species 'P' must also be reducible in the potential range where the reduction from b to c takes place.

A comparison of experimental CVs (—) and simulated ones (○–○–○) based on the ECE mechanism in (Scheme 2) is shown Fig. 3 for complex **3**. The cyclic voltammograms of the other complexes are very similar.

It should be emphasized at this point that the chemical characterization of the side product 'P' formed after the second reduction step was beyond the scope of the present paper. Nevertheless, it was necessary to examine the kinetic of the underlying decomposition reaction carefully to get the value of the energetic interaction of both metal centres (reflected in the separation of the redox potentials) we were actually interested in.

Table 1 shows the results of a systematic study executed not only for **1**, and **2**, but also for some other complexes of the type [(R–M)(**A**)(M–R)]: The value of the rate constant kf_2 was always in the range between 1×10^5 and 2×10^5 M^{-1} $s^{-}1$ for each complex and has not been reported in Table 1.

It is likely that one M(II) center is reduced first giving Ni(I) or Pd(I). However, attempts to generate and isolate such M(I) species by reducing of the oxam complexes with Na/Hg in separate Schlenk flasks were not successful.

The reduced metal species effects the electronic properties of the second one thereby shifting the reduction potential for the second charge transfer process to more negative potentials. The differences between the standard potentials of both reduction steps vary from 115 to 135 mV indicating a strong electronic communication between both redox centers. In the absence of such a mutual communication, the difference between the standard potentials should be close to the

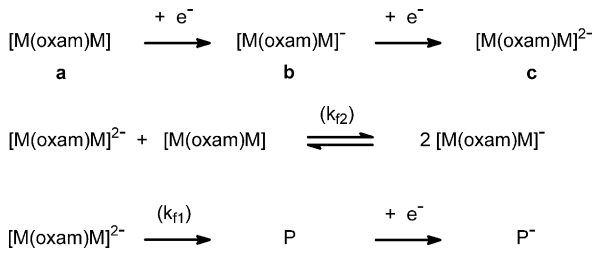

Scheme 2. Postulated mechanism for the electrochemical reduction of **1**–**7**.

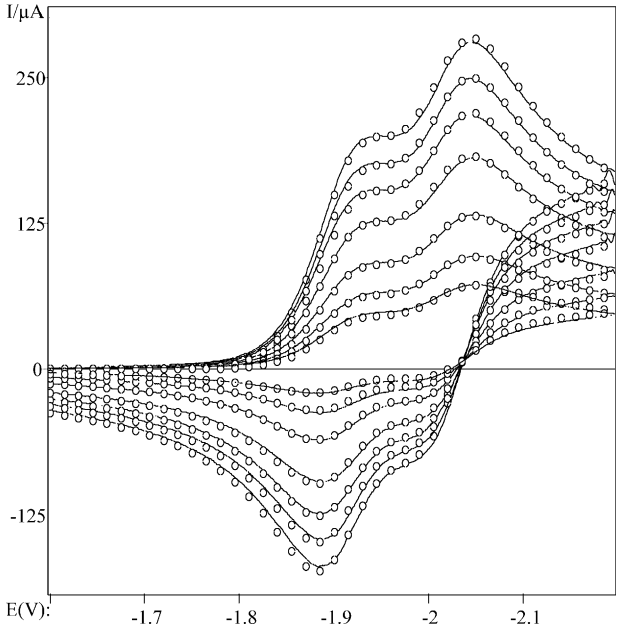

Fig. 3. Experimental (—) and simulated (○) cyclic voltammograms of complex **3** using scan rates between 10 (bottom) and 200 V s^{-1} (top).

theoretical value of 35.6 mV [22,23] reflecting the pure entropy effect. Obviously in the palladium complex **5** the electronic interaction between both redox sides is weaker than in the nickel compounds resulting in a potential difference of only 80 mV. When replacing the alkyl- or aryl ligands by acetylide and phenylacetylide (complexes **6** and **7**), the first reduction step proceeds at much more positive potentials as in the case of compounds **1**–**5**, while the potential of the second reduction step is almost unaffected. Consequently, the difference between both potentials is much larger as in the case of **1**–**5** (**6**: 380 and **7**: 375 mV). This is a clear indication for a much stronger electronic communication between both redox centres. It can also be concluded that the properties of the twofold reduced species of **6** and **7** are very similar to those of **1**–**5**, because the reduction potentials of the latter are closer together than the ones of the corresponding species formed after the first reduction step. In contrast to the alkyl- and aryl oxam complexes, the formation of the product 'P' is less preferred by **6** and **7**, as indicated by the smaller values of the rate constant kf_1 compared to those of **1**–**5**. The much more positive values of the reduction potentials associated with the first reduction of **6** and **7** compared to those of **1**–**5** may be due to the unsaturated character of the acetylide group.

Electronic communication between two redox centers in binuclear complexes continues to attract considerable attention [24–27]. For example, García-Herbosa reported about binuclear Pd(II) complexes containing 1,3-di-*p*-tolyltriazenido bridging ligands and the dependence of their redox properties on cis and trans isomerization of the two equivalent redox sides [28]. In

Table 1
Halfwave potentials and kinetic constants for the electrochemical reduction of **1**–**7** in THF + $(n\text{-Bu})_4NPF_6$

No.	R	M	E_1° (V) [a]	E_2° (V) [a]	$\Delta(E_1^\circ - E_2^\circ)$ (mV)	kf_1 (s^{-1})
1	–*n*-Bu	Ni	−1.930	−2.055	125	230
2	–*n*-Hex	Ni	−1.950	−2.070	120	35
3	$-CH_3$	Ni	−1.925	−2.040	115	40
4	–Ph	Ni	−1.865	−2.000	135	75
5	$-CH_3$	Pd	−1.970	−2.050	80	230
6	–CCH	Ni	−1.455	−1.835	380	10
7	–CCPh	Ni	−1.400	−1.775	375	10

All potentials are referenced with respect to a Ag | AgCl electrode in acetonitrile containing 0.25 M $N(n\text{-Bu})_4Cl$.
[a] Rounded to ±5 mV.

all these cases no particular attention has been paid to evaluate the electrochemistry of the complexes quantitatively using the sophisticated simulation tools available nowadays.

3. Conclusions

To the best of our knowledge, the planar oxam complexes **1** and **2** are the first binuclear Ni(II) organometallic compounds containing σ-bounded *n*-butyl- and *n*-hexyl groups, which have been characterized by mass spectrometry, elemental analysis, NMR and X-ray diffraction analysis. The molecular structures of **1** and **2** give no evidences for agostic interactions between the β- nor the γ-hydrogen atoms of the *n*-alkyl chains and the Ni center atoms. Both complexes are unusually thermally stable and only start to decompose at above 180 °C in the solid state. The thermal reaction of a mixture of **1** and **2** in toluene gives clear evidences of an intermolecular transfer mechanism of the *n*-alkyl chains.

Electrochemical studies of a number of *n*-alkyl-, aryl- and acetylide–oxam Ni(II) and Pd(II) complexes indicate that the two metal centers in the binuclear complexes communicate to each other mediated by the bridging oxam ligand. This is of general importance for those catalytic reactions of the complexes in which the two metals are catalytically active.

4. Experimental

4.1. General procedures

All manipulations were carried out by using modified Schlenk techniques under an atmosphere of argon. Prior to use, tetrahydrofurane and toluene were dried over potassium hydroxide and distilled over Na–benzophenone. Hexane solutions of *n*-butyllithium (1.6 M, Aldrich) and *n*-hexyllithium (2.5 M, Fluka) were used as received. ^1H- and ^{13}C-NMR spectra were recorded on Bruker Avance 200 and 400 spectrometers. Mass spectra were recorded on a Finnigan MAT SSQ 710. Values for *m*/*z* are for the most intense peak of isotope envelope. The measured isotopic patterns for the nickel containing species are in good agreement with the calculated isotopic pattern. Elemental analyses were performed with Leco CHNS-932. Ni analyses were carried out by titration of a solution in dilute hydrochloric acid with 0.01 M EDTA using murexid as indicator. [(acac)Ni(**A**)Ni(acac)] was prepared according to described methods [4]. DTA and DTG measurements were performed with selfmade devices.

4.1.1. Complex *1*

A solution of [(acac)Ni(**A**)Ni(acac)] (1.227 g, 1.50 mmol) in THF (120 ml) was treated with *n*-butyllithium (2.0 ml, 3.2 mmol), dissolved in hexane, dropwise at −78 °C. After stirring the solution at room temperature (r.t.) for 18 h, the solvent was removed by oil pump vacuum. The residue was extracted with toluene (60 ml). The extract was filtered and the precipitate was washed with toluene (10 ml). The unified clear solution was concentrated by oil pump vacuum (ca. 20 ml) and kept at −18 °C for 3 days. Brown crystals of **1** crystallized. After removing the mother liquid the crystals were washed with cold toluene (20 ml), pentane (20 ml) and were dried by oil pump vacuum (15 min) at r.t. Yield: 0.459 g (42%). Elemental Anal. Calc. for $C_{40}H_{52}N_6Ni_2$ ($M_w = 734.27$ g mol^{-1}): C, 65.43; H, 7.14; N, 11.45; Ni, 15.98. Found: C, 65.30; H, 7.21; N, 11.07; Ni, 15.97%. ^1H-NMR (400 MHz, benzene-d_6) δ −0.03–(−0.01) (m, 4H, CH_2, *n*-butyl α-CH_2), 0.86–0.89 (m, 6H, CH_3, *n*-butyl CH_3), 1.25–1.49 (m, 8H, CH_2, *n*-butyl β-, γ-CH_2), 2.23 (s, 6H, CH_3, *mes para*), 2.75 (s, 12H, CH, *mes ortho*), 3.76 (s, 4H, CH_2, picolyl CH_2), 5.64 (d, 2H, $^3J_{HH} = 7.8$ Hz, CH, 3-pyridyl), 6.07 (t, 2H, $^3J_{HH} = 6.4$ Hz, CH, 5-pyridyl), 6.42 (t, 2H, $^3J_{HH} = 7.6$ Hz, CH, 4-pyridyl), 6.80 (s, 4H, CH, *mes meta*), 7.90 (d, 2H, $^3J_{HH} = 5.7$ Hz, CH, 6-pyridyl). ^{13}C-NMR (50 MHz, benzene-d_6) δ 14.0 (s, CH_3, *n*-butyl), 14.6 (s, CH_2, *n*-butyl), 19.6 (s, CH_3, *mes ortho*), 21.2 (CH_3, *mes para*), 27.0 (s, CH_2, *n*-butyl), 33.0 (s, CH_2, butyl), 52.8 (s, CH_2,

picolyl CH_2), 120.4 (s, CH, 3-pyridyl), 121.9 (CH, 5-pyridyl), 128.3 (C, CH, *mes meta*), 133.1 (s, C), 134.6 (s, CH, 4-pyridyl), 135.6 (s, C), 143.9 (s, C), 144.1 (s, C), 148.3 (s, CH, 6-pyridyl), 162.6, 168.2 (s, C). ^{1}H-NMR (400 MHz, THF-d_8) δ −0.60–(−0.55) (m, 4H, CH_2, *n*-butyl α-CH_2), 0.50–0.53 (m, 6H, *n*-butyl CH_3), 0.81–0.89 (m, 4H, CH_2, *n*-butyl γ-CH_2), 0,98–1.02 (m, 4H, CH_2, *n*-butyl β-CH_2), 2.23 (s, 6H, CH_3, *mes para*), 2.45 (s, 12H, CH, *mes ortho*), 3.60 (s, 4H, CH_2, picolyl CH_2), 6.64 (d, 2H, $^3J_{HH} = 7.8$ Hz, CH, 3-pyridyl), 6.73 (s, 4H, CH, *mes meta*), 6.98 (t, 2H, $^3J_{HH} = 6.1$ Hz, CH, 5-pyridyl), 7.53 (t, 2H, $^3J_{HH} = 7.6$ Hz, CH, 4-pyridyl), 7.83 (d, 2H, $^3J_{HH} = 5.6$ Hz, CH, 6-pyridyl). ^{13}C-NMR (100 MHz, THF-d_8) δ 13.8 (CH_3, *n*-butyl CH_3), 14.1 (CH_2, *n*-butyl α-CH_2), 19.4 (CH_3, *mes ortho*), 21.1 (CH_3, *mes para*), 27.1 (CH_2, *n*-butyl γ-CH_2), 33.1 (CH_2, *n*-butyl β-CH_2), 53.2 (CH_2, picolyl CH_2), 121.4 (CH, 3-pyridyl), 123.1 (CH, 5-pyridyl), 127.7 (CH, *mes meta*), 133.6, 135.9 (C), 136.1 (CH, 4-pyridyl), 144.2 (C), 149.1 (CH, 6-pyridyl), 162.8, 169.1 (C). MS (neg. DCI/H_2O) *m*/*z*: 774, $[M+C_3H_6]^+$ (100%); 732, $[M]^+$ (44%).

4.1.2. Complex **2**

Analogously to **1**, [(acac)Ni(**A**)Ni(acac)] (1.227 g, 1.50 mmol) was reacted with a solution of *n*-hexyllithium (1.3 ml, 3.3 mmol). A golden brown crystalline solid was obtained. Yield: 0.576 g (49%). Elemental Anal. Calc. for $C_{44}H_{60}N_6Ni_2$ ($M_w = 790.38$ g mol^{-1}): C, 66.86; H, 7.65; N, 10.63; Ni, 14.85. Found: C, 66.55; H, 7.52; N, 10.41; Ni, 14.96%. ^{1}H-NMR (400 MHz, benzene-d_6) δ −0.05–(−0.01) (m, 4H, CH_2, *n*-hexyl α-CH_2), 0.90–0.93 (m, 6H, CH_3, *n*-hexyl CH_3), 1.21–1.33 (m, 12H, CH_2, *n*-hexyl γ-, δ-, ε-CH_2), 1.41–1.47 (m, 4H, CH_2, *n*-hexyl β-CH_2), 2.25 (s, 6H, CH_3, *mes para*), 2.74 (s, 12H, CH, *mes ortho*), 3.75 (s, 4H, CH_2, picolyl CH_2), 5.65 (d, 2H, $^3J_{HH} = 7.9$, CH, 3-pyridyl), 6.09 (t, 2H, $^3J_{HH} = 6.2$, CH, 5-pyridyl), 6.43 (t, 2H, $^3J_{HH} = 7.7$, CH, 4-pyridyl), 6.80 (s, 4H, CH, *mes meta*), 7.90 (d, 2H, $^3J_{HH} = 5.6$, CH, 6-pyridyl). ^{13}C-NMR (100 MHz, benzene-d_6): δ 14.5 (s, CH_3, *n*-hexyl-CH_3), 15.2 (s, CH_2, *n*-hexyl α-CH_2), 19.6 (s, CH_3, *mes ortho*), 21.2 (s, CH_3, *mes para*), 23.2 (s, CH_2, *n*-hexyl γ-, δ-, ε-CH_2), 30.6 (s, CH_2, *n*-hexyl β-CH_2), 32.0, 34.1 (s, CH_2, *n*-hexyl γ-, δ-, ε-CH_2), 52.8 (s, CH_2, picolyl CH_2), 120.4 (s, CH, 3-pyridyl), 121.9 (s, CH, 5-pyridyl), 127.6 (s, CH, *mes meta*), 133.1 (s, C), 134.1 (s, CH, 4-pyridyl), 135.6, 143.9 (s, C), 148.4 (s, CH, 6-pyridyl), 162.6, 168.2 (s, C). MS (DEI) *m*/*z*: 788, $[M]^+$ (< 0.5%); 704, $[M-C_6H_{13}+1]^+$ (0.5%); 620, $[M-2C_6H_{13}+2]^+$ (2.3%); 618, $[M-2C_6H_{13}]^+$ (1.6%).

4.2. Thermal investigations

In a typical run 0.1–0.2 mmol of **1** and **2**, respectively were heated at 200 °C for 10 min in vacuo (investigations in the liquid phase: Equimolar amounts of **1** and **2** were dissolved in toluene (2 ml) and heated at 110 °C for 30 min). After cooling the Schlenk flasks with liquid nitrogen the residues were extracted with toluene (1 ml). The solutions were analyzed by gas chromatography with the standards decane (for thermal decomposition experiments of **1** and **2** in the solid state), and tetradecane (for thermal decomposition in solution).

4.3. Cyclic voltammetry

Cyclic voltammetric measurements have been conducted in 3-electrode technique using an home-built computer controlled instrument based on the DAP-3200a data acquisition board (DATALOG Systems). The experiments were performed in THF containing 0.5M tetra-*n*-butylammonium-hexafluorophosphate under a blanket of solvent-saturated argon. The ohmic resistance, which had to be compensated for, was determined by measuring the impedance of the system at potentials where the faradaic current was negligibly small. Background correction was accomplished by subtracting the current curves of the blank electrolyte (containing the same concentration of supporting electrolyte) from the experimental CVs. The reference electrode was an Ag | AgCl electrode in acetonitrile containing 0.25M tetra-*n*-butylammonium chloride. The potential of this reference system was calibrated by measuring the potential of the ferrocenium/ferrocene couple at the end of each experiment. The latter redox couple was found to be at +0.875 V.

The working electrode was an hanging mercury drop ($m_{Hg\text{-}drop} = 3.95$–4 mg) produced by the CGME (Bioanalytical Systems, Inc., West Lafayette, USA).

4.4. Crystal structure determination

The intensity data for the compound **1** were collected on a Nonius CAD4 diffractometer and for the compound **2** on a Nonius Kappa CCD diffractometer, using graphite-monochromated Mo–K_α radiation. Data were corrected for Lorentz and polarization effects, but not for absorption [29–31].

The structures were solved by direct methods (SHELXS [32]) and refined by full-matrix least-squares techniques against F_o^2 (SHELXL-97 [33]). The hydrogen atoms of the structures were included at calculated positions with fixed thermal parameters. All non-hydrogen atoms were refined anisotropically [33]. XP (Siemens Analytical X-ray Instruments Inc.) was used for structure representations.

4.4.1. Crystal data for **1**

$C_{49}H_{52}N_6Ni_2 \cdot 5/3C_7H_8$, $M_r = 887.85$ g mol^{-1}, brown prism, size 0.18 × 0.16 × 0.10 mm^3, triclinic, space group $P\bar{1}$, $a = 11.518(3)$, $b = 16.283(3)$, $c = 19.753(6)$ Å, $\alpha = 98.57(3)$, $\beta = 91.67(3)$, $\gamma = 103.68(4)°$, $V = 3551(1)$ Å^3, $T = -90$ °C, $Z = 3$, $\rho_{calc} = 1.245$ g cm^{-3}, μ(Mo–K_α) =

8.36 cm^{-1}, F(000) = 1420, 16727 reflections in $h(-14/14)$, $k(0/21)$, $l(-25/25)$, measured in the range $2.49 \leq \Theta \leq 27.43^{\circ}$, completeness $\Theta_{max} = 99.8\%$, 16 156 independent reflections, $R_{int} = 0.018$, 10540 reflections with $F_o > 4\sigma(F_o)$, 732 parameters, two restraints, $R_{1\ obs} = 0.061$, $wR_{2\ obs} = 0.179$, $R_{1\ all} = 0.116$, $wR_{2\ all} = 0.209$, GOF = 1.053, largest difference peak and hole: 1.055/ −1.112 e $Å^{-3}$.

4.4.2. Crystal data for 2

$C_{44}H_{60}N_6Ni_2 \cdot 1/4C_4H_8O$, $M_r = 808.43$ g mol^{-1}, brown prism, size $0.10 \times 0.10 \times 0.03$ mm^3, orthorhombic, space group *Pbcn*, $a = 47.967(3)$, $b = 11.2398(6)$, $c = 16.3960(8)$ Å, $V = 8839.7(8)$ $Å^3$, $T = -90$ °C, $Z = 8$, $\rho_{calc} = 1.215$ g cm^{-3}, $\mu(Mo–K_\alpha) = 8.89$ cm^{-1}, $F(000) = 3456$, 28 307 reflections in $h(-45/57)$, $k(-13/8)$, $l(-10/19)$, measured in the range $2.21 \leq \Theta \leq 25.35^{\circ}$, completeness $\Theta_{max} = 97.6\%$, 7902 independent reflections, $R_{int} = 0.158$, 3806 reflections with $F_o > 4\sigma(F_o)$, 479 parameters, zero restraints, $R_{1\ obs} = 0.103$, $wR_{2\ obs} = 0.220$, $R_{1\ all} = 0.2212$, $wR_{2\ all} = 0.274$, GOF = 1.044, largest difference peak and hole: 0.970/ −0.717 e $Å^{-3}$.

5. Supplementary material

Crystallographic data for the structural analysis have been deposited with the Cambridge Crystallographic Data Centre, CCDC nos. 214426 and 214427. Copies of this information may be obtained free of charge from The Director, CCDC, 12 Union Road, Cambridge CB2 1EZ, UK (Fax: +44-1223-336033; e-mail: deposit@ccdc.cam.ac.uk or www: http://www.ccdc.cam.ac.uk).

References

[1] T. Döhler, H. Görls, D. Walther, J. Chem. Soc. Chem. Commun. (2000) 945.
[2] D. Walther, T. Döhler, N. Theyssen, H. Görls, Eur. J. Inorg. Chem. (2001) 2049.
[3] D. Zhang, G.-X. Jin, Organometallics 22 (2003) 2851.
[4] D. Walther, M. Stollenz, L. Böttcher, H. Görls, Z. Anorg. Allg. Chem. 627 (2001) 1560.
[5] S. Rau, L. Böttcher, S. Schebesta, M. Stollenz, H. Görls, D. Walther, Eur. J. Inorg. Chem. (2002) 2800.
[6] D. Walther, M. Stollenz, H. Görls, Organometallics 20 (2001) 4221.
[7] K. Lamm, M. Stollenz, M. Meier, H. Görls, D. Walther, J. Organomet. Chem. 681 (2003) 24.
[8] P. Voth, S. Arndt, T.P. Spaniol, J. Okuda, L.J. Ackerman, M.L.H. Green, Organometallics 22 (2003) 65.
[9] D.J. Anderson, R. Eisenberg, Inorg. Chem. 33 (1994) 5378.
[10] O. Boutry, A. Gutierrez, A. Monge, M.C. Nicasio, P.J. Perez, E. Carmona, J. Am. Chem. Soc. 114 (1992) 7288.
[11] E. Gutierrez-Puebla, A. Monge, M.C. Nicasio, P.J. Perez, M.L. Poveda, E. Carmona, Chem. A Eur. J. 4 (1998) 2225.
[12] A. Sebald, B. Wrackmeyer, C.B. Theocharis, W. Jones, J. Chem. Soc. Dalton Trans. (1984) 747.
[13] T.G. Gardner, G.S. Girolami, J. Chem. Soc. Chem. Commun. (1987) 1758.
[14] E.G. Thaler, K. Folting, J.C. Huffman, K.G. Caulton, J. Organomet. Chem. 376 (1989) 343.
[15] A.C. Filippou, S. Schneider, Organometallics 22 (2003) 3010.
[16] L.-C. Liang, J.-M. Lin, C.-H. Hung, Organometallics 22 (2003) 3007.
[17] T.O. Northcutt, D.D. Wick, A.J. Vetter, W.D. Jones, J. Am. Chem. Soc. 123 (2001) 7257.
[18] P. Ellis, J.M. Pearson, A. Haynes, H. Adams, N.A. Bailey, P.M. Maitlis, Organometallics 13 (1994) 3215.
[19] B. Köhler, M. Knauer, W. Clegg, M.R.J. Elsegood, B.T. Golding, J. Rétey, Angew. Chem. 107 (1995) 2580.
[20] P. Xiang, Y. Chen, X.-J. Shen, H.-L. Chen, C.-Y. Duan, Acta Crystallogr. Sect. C 56 (2000) 421.
[21] M. Rudolph, S.W. Feldberg, DigiSim® 3.0 Software, Bioanalytical Systems Inc., West Lafayette, IN 47906, USA, 2001.
[22] F. Ammar, J.-M. Saveant, J. Electroanal. Chem. 47 (1973) 215.
[23] J.B. Flanagan, S. Margel, A.J. Bard, F.C. Anson, J. Am. Chem. Soc. 100 (1978) 4248.
[24] M. Haga, T. Matsumara-Inoue, S. Yamabe, Inorg. Chem. 26 (1987) 4148.
[25] A. Klein, W. Kaim, F.M. Hornung, J. Fiedler, S. Zalis, Inorg. Chim. Acta 264 (1997) 269.
[26] M. Beley, J.-P. Collin, R. Louis, B. Metz, J.-P. Sauvage, J. Am. Chem. Soc. 113 (1991) 8521.
[27] P. Steenwinkel, D.M. Grove, N. Feldman, A.L. Spek, G. van Koten, Organometallics 17 (1998) 5647.
[28] G. García-Herbosa, N.G. Connely, A. Muñoz, J.V. Cuevas, A.G. Orpen, S.D. Politzer, Organometallics 20 (2001) 3223.
[29] MOLEN, An Interactive Structure Solution Procedure, Enraf–Nonius, Delft, The Netherlands, 1990.
[30] COLLECT, Data Collection Software; Nonius B.V., The Netherlands, 1998.
[31] Z. Otwinowski, W. Minor, Processing of X-ray diffraction data collected in oscillation mode, in: C.W. Carter, R.M. Sweet (Eds.), Methods in Enzymology: Macromolecular Crystallography, Part A, vol. 276, Academic Press, New York, 1997, pp. 307–326.
[32] G.M. Sheldrick, Acta Crystallogr. Sect. A 46 (1990) 467.
[33] G.M. Sheldrick, SHELXL-97, University of Göttingen, Germany, 1997.